

DEUTSCHES ELEKTRONEN-SYNCHROTRON DESY

DESY 77/07
January 1977



Small-Angle Photon Scattering on Complex Nuclei

by

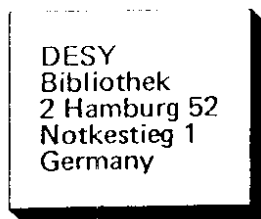
L. Criegee, G. Franke, A. Giese, Th. Kahl, G. Poelz, U. Timm,
H. Werner and W. Zimmermann

Abstract:

Photons of 3 GeV and 5 GeV were scattered on 7 different elements, ranging from Be to Au, and detected with a pair spectrometer. The angular distributions show diffractive patterns consistent with known nuclear sizes. Forward cross sections are 20-30% lower than expected from an A^2 dependence. This shadowing effect is qualitatively explained by photon interactions via intermediate hadronic states.

2 HAMBURG 52 · NOTKESTIEG 1

To be sure that your preprints are promptly included in the
HIGH ENERGY PHYSICS INDEX ,
send them to the following address (if possible by air mail) :



Small-Angle Photon Scattering on Complex Nuclei

by

L.Criegee, G.Franke, A.Giese, Th.Kahl, G.Poelz, U.Timm, H.Werner, W.Zimmermann
Deutsches Elektronen-Synchrotron DESY, Hamburg, Germany

Abstract

Photons of 3 GeV and 5 GeV were scattered on 7 different elements, ranging from Be to Au, and detected with a pair spectrometer. The angular distributions show diffractive patterns consistent with known nuclear sizes. Forward cross sections are 20-30% lower than expected from an A^2 dependence. This shadowing effect is qualitatively explained by photon interactions via intermediate hadronic states.

Diffraction scattering of photons on nuclear targets gives information on two interesting problems: First, the width of the diffraction peak tells whether photons 'see' the same nuclear sizes as other projectiles. Secondly, the forward intensity is related to the absorption of photons in nuclear matter. Due to the small photon-nucleon cross section one would expect absorption to be negligible, and therefore a total cross section rising like the mass number A , and a forward cross section proportional to A^2 .

In contrast to the latter expectation, several measurements of the total cross section on nuclei have demonstrated a slower rise^{1,2,3)}. This deficiency has been called shadowing and can be explained by assuming that the photons passing the nucleus are converted part of the time into hadronic states with a short mean free path. If this picture is correct, the effect should also be seen in the total scattering cross section for virtual photons of small q^2 . Several measurements⁴⁾ were, however, consistent with no shadowing.

In view of this unclear situation we have performed an experiment in which real photons of 3 and 5 GeV were scattered elastically on various nuclei. We have determined the cross sections in the kinematic regions $0.001 \leq |t| \leq 0.020$ (GeV/c)² and $0.002 \leq |t| \leq 0.060$ (GeV/c)² respectively, and extrapolated to $t = 0$. Since the forward scattering cross section is roughly proportional to A^2 , the sensitivity for shadowing effects should be twice as large as in total cross sections measurements.

The data were taken at the DESY Electron-Synchrotron with the aid of an experimental setup used before in a Compton experiment on protons and deuterons which is described in the preceding paper⁵⁾. The liquid target was replaced by foils of Be, C, Al, Ti, Cu, Ag or Au, of typically 0.04 R.L. thickness. The pair spectrometer which analysed the scattered photons had an energy resolution of 1.3 % and 1.8 % fwhm at 5 and 3 GeV.

The analysis of the data is very similar to that for the proton and deuteron data⁵⁾. The rate of accidental pairs was smaller than 3 %. An empty target rate of 3 to 15 %, depending on the scattering angle was subtracted. Corrections for multiple track events (1.3 %) were applied. Contributions from 'inelastic' reactions, like π^0 -photoproduction, were separated by means of the different shape in the photon spectrum they produce. While the elastically scattered photons reproduce the step spectrum of the primary beam, the spectrum of inelastic processes vanishes smoothly towards the maximum energy. Fig. 1 demonstrates the different shapes and shows the result of a computer fit by which both were separated.

The inelastic reactions considered are the same as in the case of protons and deuterons, namely $\gamma A \rightarrow \pi^0 A$ and $\gamma A \rightarrow nA$ with $\pi^0 \rightarrow \gamma\gamma$, $n \rightarrow \omega\omega$ with $\omega \rightarrow Y\pi^0$ 8) and $\gamma A \rightarrow \gamma A + m\pi$ ($m \geq 1$) 9), as well as resonance production at single nucleons $\gamma N \rightarrow \gamma N^*$ with $N^*(1470)$, $N^*(1520)$ and $N^*(1688)$ 9).

The contributions from all these reactions were computed from the

corresponding proton cross sections, assuming total incoherence over the nucleus, and added up to one representative background spectrum. This background as well as the calculated Compton spectrum were corrected for acceptance by Monte-Carlo calculations. The measured spectrum was then decomposed into the two contributions by a linear fit, separate in each t -bin.

The resulting t -dependence of the elastic cross sections is shown in figs. 2a and 2b for the two energies and several targets used. The data at 5 GeV show a diffraction pattern with indications of a first minimum for nuclei heavier than Cu ($A = 64$). The curves were obtained from an optical model calculation in the following way: The main contribution is the coherent cross section $\frac{d\sigma}{dt} \Big|_{coh}(t)$, calculated by including direct photon scattering as well as the contributions of intermediate p , ω , and ϕ mesons¹⁵⁾. The agreement at high t is improved by adding an incoherent cross section $\frac{\lambda}{A} \left(\frac{d\sigma}{dt} \Big|_{coh}(0) - \frac{d\sigma}{dt} \Big|_{coh}(t) \right)$ which vanishes at $t = 0$. The empirical constant was chosen as $\lambda = 1/2$. The sum of both contributions was fitted to the low- t points (solid in fig. 2a), with an overall scale and the nuclear radius (Wood-Saxon) as free parameters.

The nuclear radii obtained in this way are shown in fig. 3. The dotted line shows for comparison the formula¹⁰⁾

$$r_A = 1.123 A^{1/3} - 0.8 A^{-1/3} r_m$$

based on tabulated values¹¹⁾. The agreement demonstrates that high energy photons see essentially the same nuclear sizes as high energy electrons.

The forward cross sections obtained from the fits are listed in table 1 with their statistical errors. The systematic errors were estimated by varying (1) the incoherent contribution, from $\lambda = 0$ to 1, (2) the converter position by 0.25 mm, corresponding to a shift of the forward angles of 0.06 mrad, (3) the measured photon energy by one standard deviation, corresponding to 4 MeV, and (4) the shape of the inelastic background. These errors have been added quadratically in the table. Normalization errors quoted result mainly from the uncertainty in target thickness, which is typically 0.5 % but rises up to 1.9 % for Au, and in the absolute quantameter calibration ($\pm 1.2 \%$).

A comparison with equivalent experimental data is obtained by calculating the total cross section from our data via the optical theorem. The phases, α , where

$$\alpha = \frac{\text{Re } f_{el}(0)}{\text{Im } f_{el}(0)}$$

of the elastic photon nucleus scattering amplitudes were calculated in an optical model¹⁴⁾. The values and their estimated errors depending on the uncertainties in the model parameters are listed in table 2. Fig. 4a and 4b show the result of this calculation. The error bars include statistical and estimated phase errors. The agreement with total cross section measurements is good. For comparison the dashed line represents the total cross section expected if it varied proportionally to A (no shadowing).

The shadowing effect can be expressed by the ratio R^2 of the measured forward cross section to the one expected for scattering on A nucleons, or by the 'effective' mass number A_{eff}/A :

$$R^2 \equiv (A_{eff}/A)^2 = \frac{d\sigma(0)_A}{d\sigma(0)_N} / (A^2 \frac{d\sigma(0)_A}{d\sigma(0)_N})$$

The cross section of the 'average' nucleon is obtained from that on the proton and neutron, assuming full coherence, by

$$\frac{d\sigma(0)_N}{d\sigma(0)_p} = \left(\frac{Z}{A} \left(\frac{d\sigma(0)_p}{d\sigma(0)_N} \right)^{1/2} + \frac{A-Z}{A} \left(\frac{d\sigma(0)_N}{d\sigma(0)_p} \right)^{1/2} \right)^2$$

As we have measured the proton Compton cross section with the same experimental set up at 5 GeV, but not at 3 GeV beam energy, the one nucleon cross sections for both energies were computed from total cross section measurements via the optical theorem and dispersion relations¹³⁾. The values used are $\frac{d\sigma(0)_p}{d\sigma(0)_N} = 1.09$ and $0.91 \mu\text{b}/(\text{GeV}/c)^2$ at 3 and 5 GeV, and $\frac{d\sigma(0)_N}{d\sigma(0)_p} = 0.84$ and $0.79 \mu\text{b}/(\text{GeV}/c)^2$ respectively. The values of R^2 obtained with this normalization are shown in fig. 5a and 5b both with statistical errors. If we use at 5 GeV our measured value $\frac{d\sigma(0)_p}{d\sigma(0)_N} = 0.82 \mu\text{b}/(\text{GeV}/c)^2$, R^2 would be increased by 10 %, leading to a shadowing of about 25 % for heavy nuclei.

For comparison results of VDM calculations are shown^{14,15)}. The full curve is obtained using the parameters listed in tab. 3. The theoretical prediction is in qualitative agreement with the data. It is however sensitive to the exact

values of the model parameters. A somewhat better quantitative agreement can be obtained for instance by changing α_{pN} to 25 mb (dashed curve) or by taking $\alpha_{pN} = -0.2$ (not shown). Inclusion of heavier vector-mesons has negligible influence at our energies¹⁶). Another way of improving the agreement consists in including in the amplitude a 20 % contribution of short-range interactions, which is not subject to shadowing^{2,15)}.

In conclusion, we have observed angular distributions which are dominated by a forward diffraction peak. They are well described by the sum of a coherent part, calculated in an optical model, and a small incoherent contribution. Nuclear radii determined from the width of the coherent peak agree with those from electron scattering. Our forward cross sections are consistent with measured total cross sections. They show 20-30 % shadowing. The shadowing effect is in qualitative agreement with VDM calculations, in particular in view of the predicted A dependence, the energy dependence, however, appears to be weaker.

We are indebted to Dr. R. Spital (Cornell University) for giving and explaining to us his photon scattering program on which our optical model calculations were based,

Literature:

- 1) V.Haynen et al., Phys.Lett. 34B, 651 (1971)
- 2) D.O.Caldwell et al., Phys.Rev. D1, 1362 (1973)
- 3) G.R.Brookes et al., Phys.Rev. D8, 2820 (1973)
- 4) W.R.Ditzler et al., Phys.Lett. 57B, 201 (1975)
- 5) S.Stein et al., SLAC-PUB 1528, (1975)
- 6) M.Braunschweig et al., Nucl.Phys. B20, 191 (1970) and private communication
- 7) M.Braunschweig et al., Phys.Lett. 33B, 236 (1970)
- 8) J. Ballam et al., SLAC-PUB 852 (1971)
- 9) G. Wolf, DESY 70/45 (1970) and private communication
- 10) L.R.B.Elton, Nuclear Sizes, Oxford Univ.Press (1961)
- 11) L.R.B.Elton, in Landolt-Börnstein, New Serien, Group I, 2, (1967)
- 12) G.Wolf, in proc. 5th Int. Symp. on Electr. & Phot. Int. at High En., Cornell University (1971)
- 13) M.Damaskos, F.J.Gilman, Phys.Rev. 1D, 1319 (1970)
- 14) K.Gottfried, D.R.Yennie, Phys.Rev. 182, 1595 (1969)
- 15) R.Spital, Cornell University, private communication and paper to be published
- 16) D.Schildknecht, Nucl.Phys. B66, 398 (1973)

We wish to thank H.Marxen and his crew for their help in constructing the spectrometer and setting up the experiment. The assistance of the members of the Hallendienst, of the Synchrotron group and of the Rechenzentrum is gratefully acknowledged.

Table 1 - Differential forward cross sections for elastic photon nucleus scattering

5 GeV	A	$d\sigma/dt$ μb/(GeV/c) ²	stat. error	syst. error	norm. error
9	53.1	5.0 %	3.01 %	1.63 %	
12	92.6	4.9	2.94	1.60	
27	405.0	4.4	5.58	1.61	
49	1220.0	3.8	5.62	1.60	
64	2032.0	4.8	3.21	1.65	
109	6121.0	3.8	3.13	1.99	
197	20630.0	8.5	3.29	2.51	
3 GeV					
9	62.9	4.3 %	2.20 %	1.60 %	
12	111.9	6.1	2.68	1.60	
27	523.0	3.5	2.72	1.72	
64	2664.0	19.0	2.80	1.65	
109	8426.0	3.6	4.19	2.04	

Table 2 - Phases $\alpha = \frac{\text{Re } f_{e1}(0)}{\text{Im } f_{e1}(0)}$ of the elastic photon nucleus scattering amplitude as given by VDM calculation¹⁶⁾ and estimated errors Δα

5 GeV	$\alpha = \frac{\text{Re } f_{e1}(0)}{\text{Im } f_{e1}(0)}$	$\Delta\alpha$	$\alpha = \frac{\text{Re } f_{e1}(0)}{\text{Im } f_{e1}(0)}$	$\Delta\alpha$
Be	-0.33	.04	Be	-.04
C	-0.34	.04	C	-.04
Al	-0.39	.05	Al	-.05
Ti	-0.44	.05	Ti	-.05
Cu	-0.46	.06	Cu	-.05
Ag	-0.51	.07	Ag	-.05
Au	-0.57	.07	Au	-.05

Table 3 - Parameters used for the VDM calculation. The total cross sections were calculated as in Ref. 16.

	$\gamma_V^2/4\pi$	$\sigma_{VN} (\mu b)$	α_{VN}
ρ	0.64	31.0	.29, .2
ω	4.6	27.5	.25, .25
φ	2.9	10.8	.1, -.25

Figure Captions:

Fig. 1 Reconstructed energy spectrum of photons scattered on Ag at 5 GeV with $0.002 \leq |t| \leq 0.04 (\text{GeV}/c)^2$.

The contributions of inelastic and Compton reactions are separated by a fit described in the text.

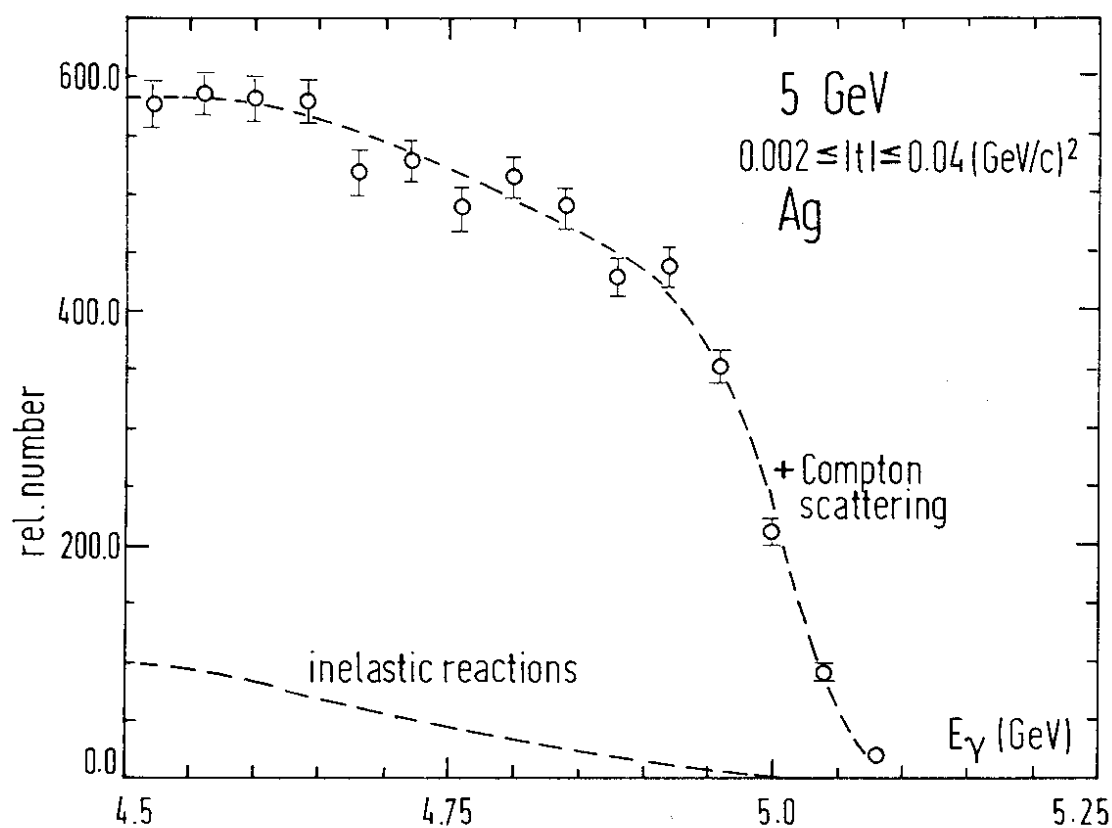
Fig. 2 Differential Compton cross sections on heavy nuclei at 5 GeV and 3 GeV photon energy.

Fig. 3 Nuclear radii (half density radii of the Woods-Saxon distribution) as measured in Compton scattering. Also shown is an interpolation curve through electron scattering data.

Fig. 4 Total photon nucleus cross sections as calculated from Compton data, compared with measured total cross sections. The dashed line is the prediction if no shadowing occurred, i.e. $\sigma^{\text{tot}}(A) = A \cdot \sigma^{\text{tot}}(N)$, where $\sigma^{\text{tot}}(N)$ is 136 and 127 μb at 3 GeV and 5 GeV respectively.

Fig. 5 Shadowing in Compton scattering at 3 GeV and 5 GeV represented by the ratio $R^2 = d\sigma/dt(0)_A / \left(2 \sqrt{d\sigma/dt(0)_p + N \sqrt{d\sigma/dt(0)_n}} \right)^2$.

Fig.1 Reconstructed Photon Energy Spectrum



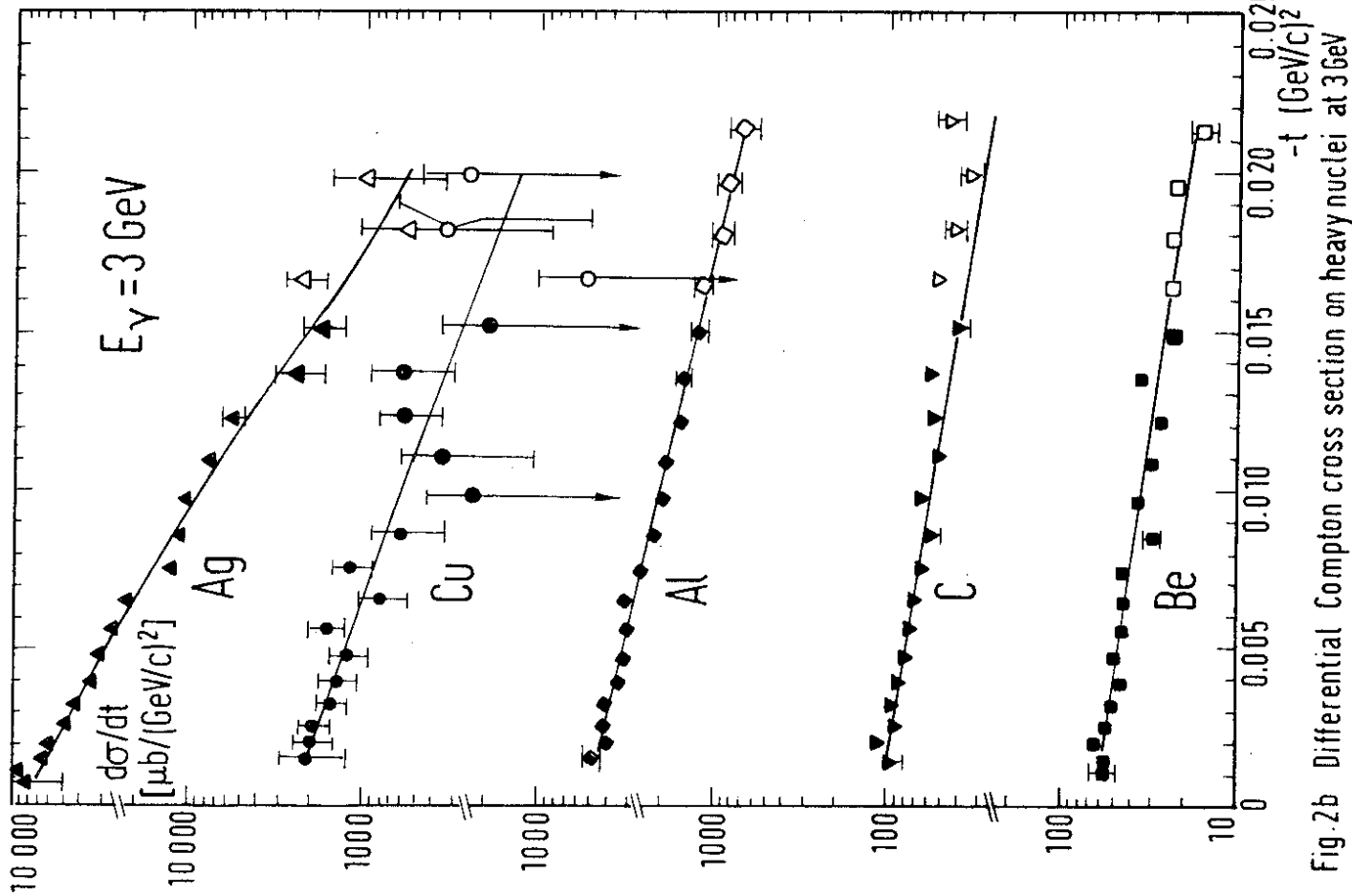


Fig.2a Differential Compton cross section on heavy nuclei at 5 GeV

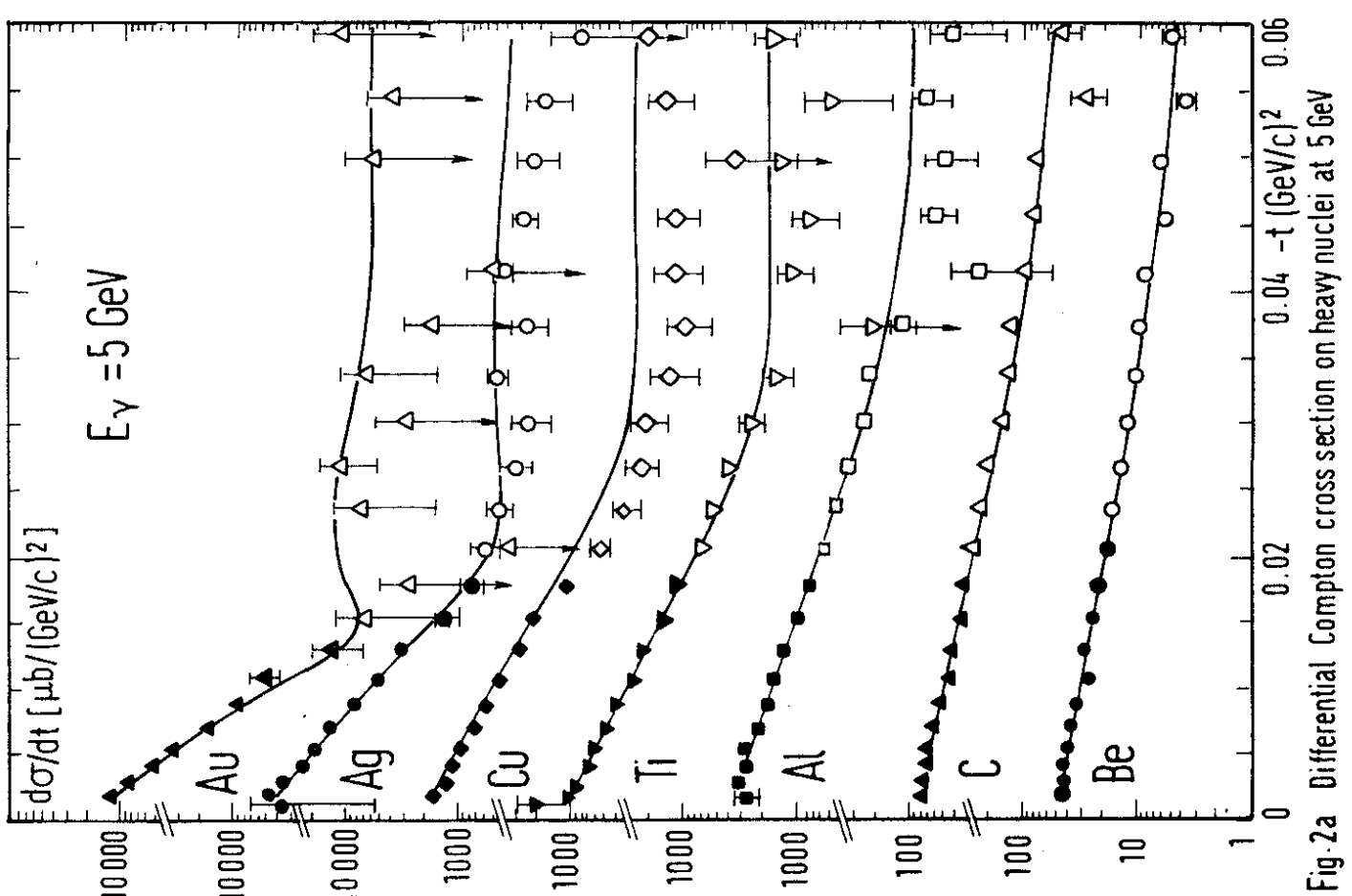


Fig.2b Differential Compton cross section on heavy nuclei at 3 GeV

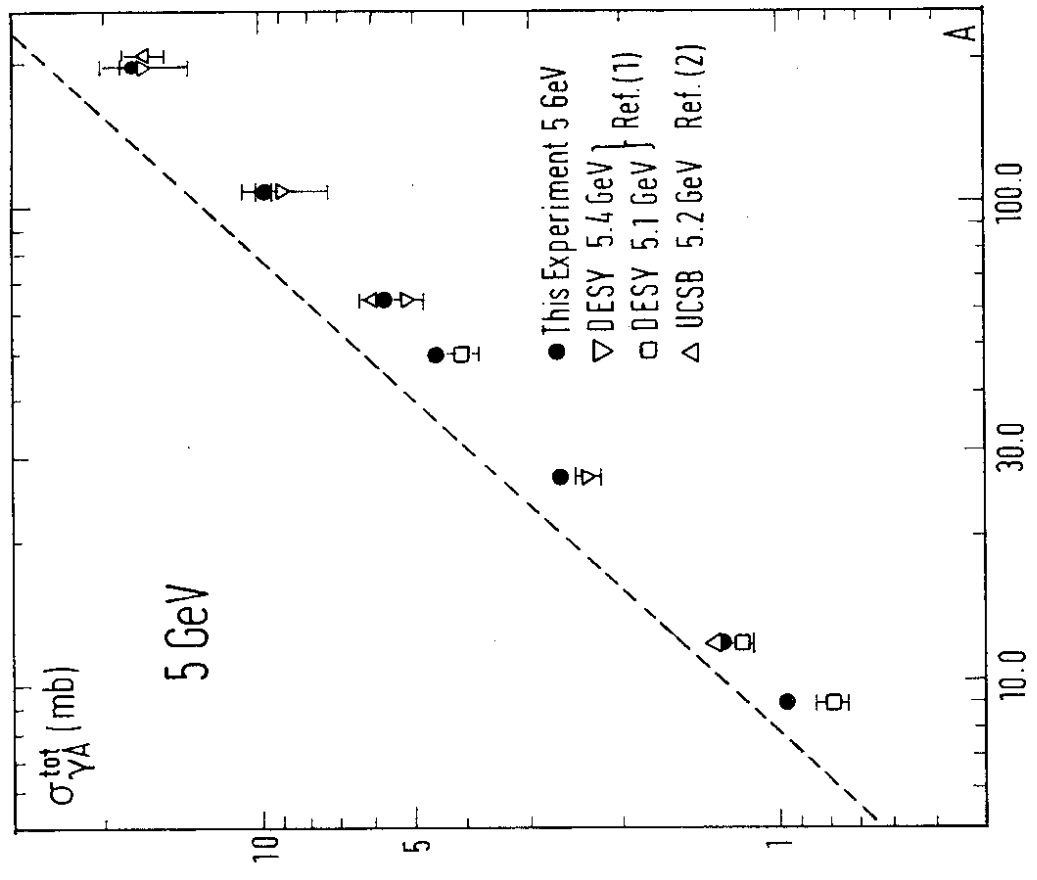


Fig.4a Total Photon Nucleus Cross Section at 5 GeV

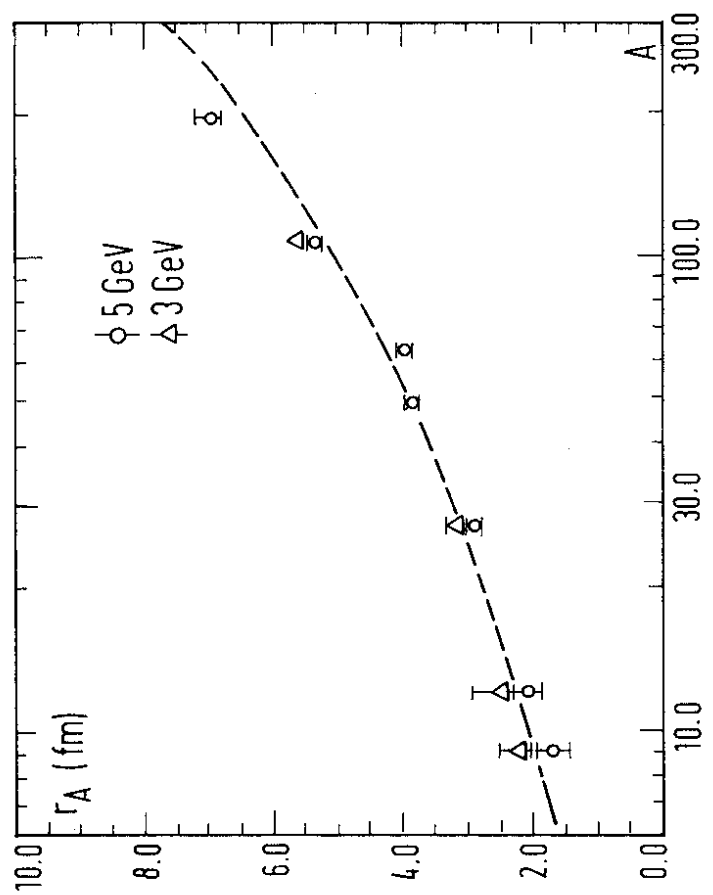


Fig.3 Nuclear Radii from Compton Scattering

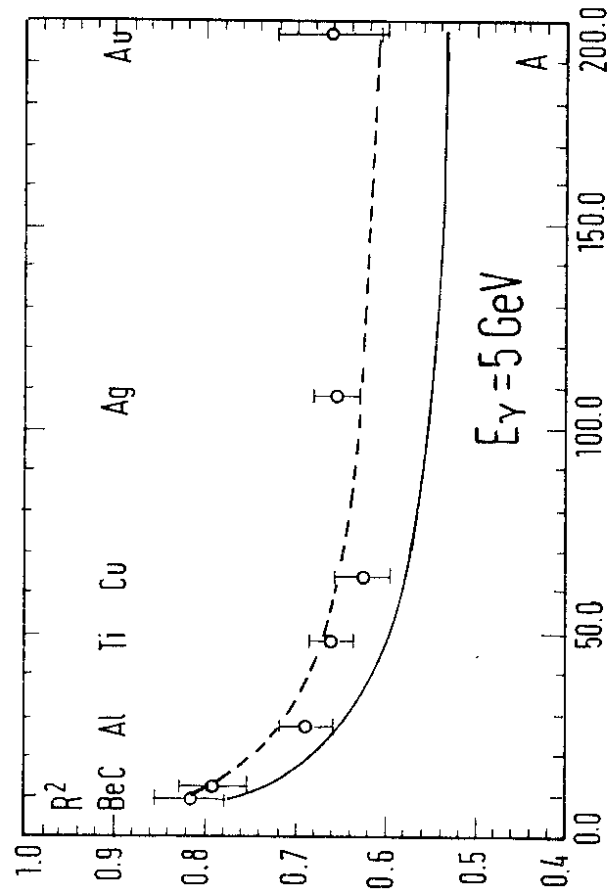


Fig. 5a Shadowing in Compton Scattering at 5 GeV

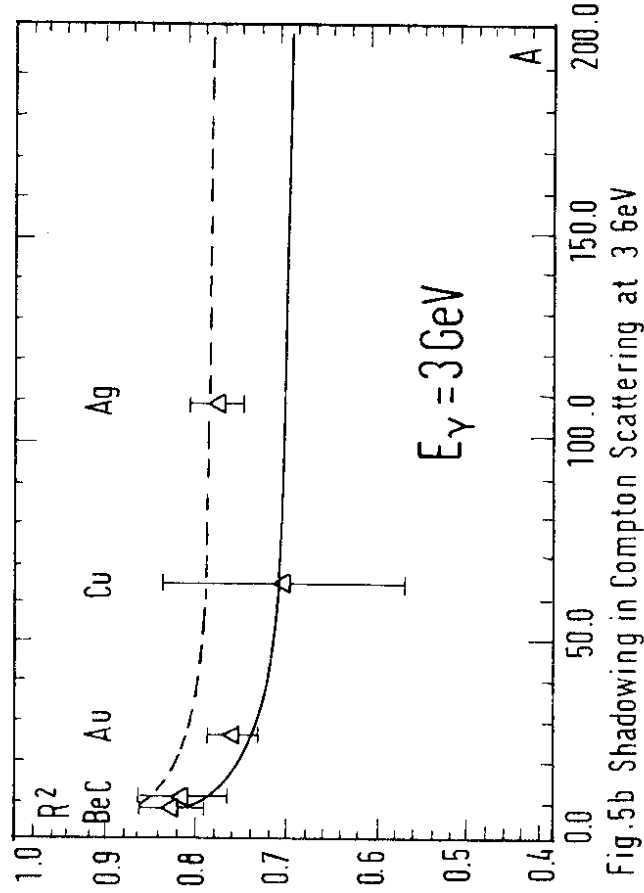


Fig. 5b Shadowing in Compton Scattering at 3 GeV

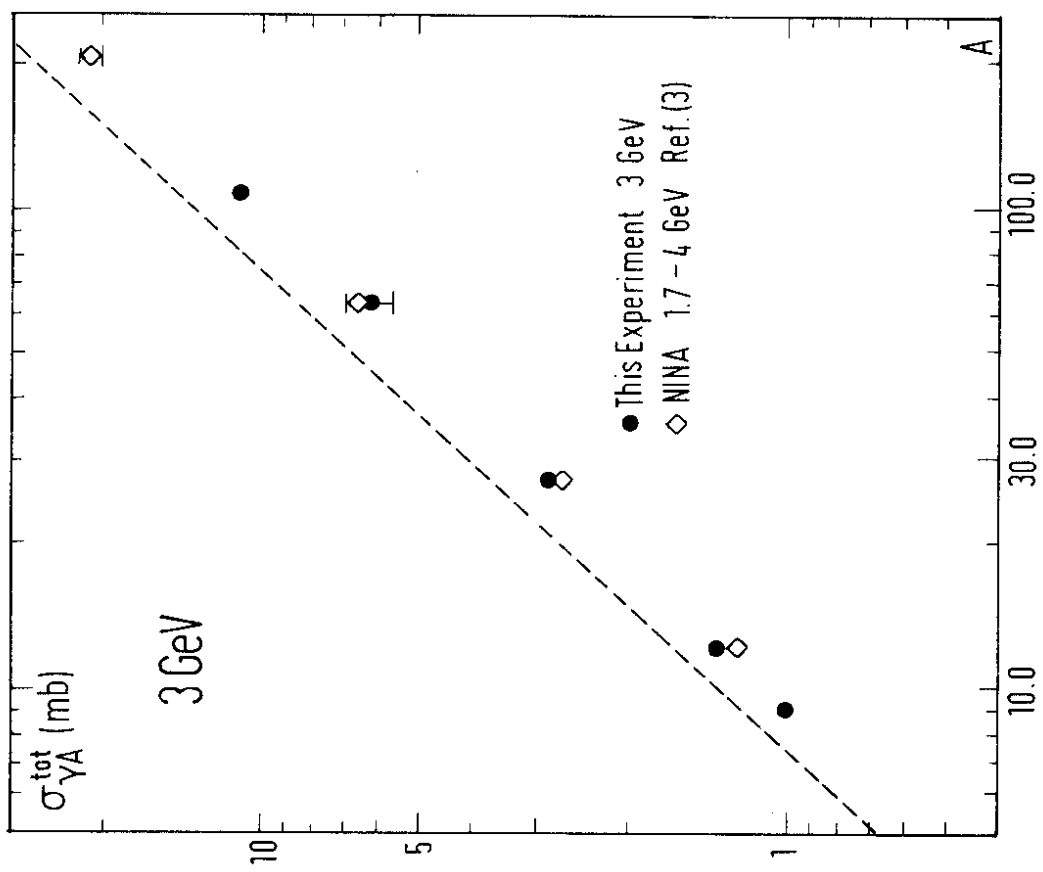


Fig. 4b Total Nucleus Cross Section at 3 GeV